HHS Public Access

Author manuscript

Ophthalmic Surg Lasers Imaging Retina. Author manuscript; available in PMC 2016 January 14.

Published in final edited form as:

Ophthalmic Surg Lasers Imaging Retina. 2014 ; 45(6): 496–505. doi:10.3928/23258160-20141118-03.

Ultrahigh-Speed Swept-Source OCT Angiography in Exudative AMD

Eric Moult, BS, **WooJhon Choi, PhD**, **Nadia K. Waheed, MD**, **Mehreen Adhi, MD**, **ByungKun Lee, MEng**, **Chen D. Lu, MS**, **Vijaysekhar Jayaraman, PhD**, **Benjamin Potsaid, PhD**, **Philip J. Rosenfeld, MD, PhD**, **Jay S. Duker, MD**, and **James G. Fujimoto, PhD**

Massachusetts Institute of Technology, Department of Electrical Engineering and Computer Science, and Research Laboratory of Electronics, Cambridge, Massachusetts (EM, WC, BL, CDL, BP, JGF); Harvard-MIT Division of Health Sciences and Technology, Cambridge, Massachusetts (EM); Tufts University Medical Center, New England Eye Center, Boston, Massachusetts (NKW, MA, JSD); Praevium Research, Santa Barbara, California (VJ); Advanced Imaging Group, Thorlabs., Newton, New Jersey (BP); and University of Miami Miller School of Medicine, Bascom Palmer Eye Institute, Department of Ophthalmology, Miami, Florida (PJR)

Abstract

Background and Objective—To investigate the potential of ultrahigh-speed swept-source optical coherence tomography angiography (OCTA) to visualize retinal and choroidal vascular changes in patients with exudative age-related macular degeneration (AMD).

Patients and Methods—Observational, prospective cross-sectional study. An ultrahigh-speed swept-source prototype was used to perform OCTA of the retinal and choriocapillaris microvasculature in 63 eyes of 32 healthy controls and 19 eyes of 15 patients with exudative AMD. Main outcome measure: qualitative comparison of the retinal and choriocapillaris microvasculature in the two groups.

Results—Choroidal neovascularization (CNV) was clearly visualized in 16 of the 19 eyes with exudative AMD, located above regions of severe choriocapillaris alteration. In 14 of these eyes, the CNV lesions were surrounded by regions of choriocapillaris alteration.

Conclusion—OCTA may offer noninvasive monitoring of the retinal and choriocapillaris microvasculature in patients with CNV, which may assist in diagnosis and monitoring.

Introduction

Exudative age-related macular degeneration (AMD), a pathology characterized by choroidal neovascularization (CNV), is a leading cause of vision loss and impairment in developed countries. Optical coherence tomography (OCT) has proven to be a valuable tool for imaging anatomic changes associated with accumulation and resolution of macular fluid in

Address correspondence to James G. Fujimoto, PhD, Massachusetts Institute of Technology, Room 36-361, 77 Massachusetts Avenue Cambridge, MA 02139; 617-253-8528; fax: 617-253-9611; jgfuji@mit.edu.

Dr. Duker did not participate in the editorial review of this manuscript. Mr. Moult and Dr. Choi contributed equally to this manuscript.

The remaining authors have no financial or proprietary interest in the materials presented herein.

patients with CNV, both before and after treatment with inhibitors of vascular endothelial growth factor (VEGF).[1-4] Until recently, OCT has been unable to visualize the pathological vascularization that is the hallmark of exudative age related macular degeneration (AMD).[5,6] Instead, fluorescein angiography (FA) and indocyanine green angiography (ICGA) have been the clinical modalities used to image neovascularization in the retina and choroid.[7,8]

Exudative AMD results from abnormal growth of choroidal blood vessels through Bruch's membrane and into the sub–retinal pigment epithelium (RPE) and subretinal space. The abnormal vasculature associated with exudative AMD can cause severe vision loss. Fortunately, the introduction of anti-VEGF medications has greatly improved the prognosis for patients with exudative AMD.[9-15] While fluorescein angiography (FA) allows visualization of CNV lesions, visualization of the choriocapillaris and choroid using FA is hindered by two properties of fluorescein: (1) its blue-green excitation wavelength is partially absorbed by the macular xanthophyll and RPE, and (2) approximately 20% of the injected fluorescein does not bind to albumin and is free to leak out of the choriocapillaris fenestrations, which creates diffuse hyperfluorescence, obscuring the vasculature.[16] In contrast, ICGA allows visualization of choroidal circulation because its near-infrared excitation wavelengths are not as readily absorbed by the macular xanthophyll and RPE, and approximately 98% of the injected indocyanine green is bound to plasma protein, preventing it from leaking out of the choriocapillaris fenestrations.[16] ICGA has also been shown to be capable of visualizing the choriocapillaris circulation.[17] However, because ICGA is not depth-resolved, the task of separating choriocapillaris blood flow from that of deeper choroidal vasculature is complex and may only be possible if it is assumed that the blood flow velocity of the larger choroidal arteries is small compared to that of the choriocapillaris.[17,18]

Histopathologic studies in patients with CNV have shown that the lesions are associated with regions of normal RPE.[19-21] The area of choriocapillaris loss extends beyond the area of CNV and it has been hypothesized that choriocapillaris degeneration results in ischemia in the RPE, which in turn causes the RPE to produce angiogenic factors that stimulate neovascularization.[19] While OCT studies have investigated choroidal thickness in exudative AMD,[22,23] current-generation OCT imaging provides insufficient detail to visualize in vivo the choroidal changes associated with exudative AMD.

OCT angiography (OCTA) is a recently developed imaging technique that generates three-dimensional microvascular angiograms in vivo, rapidly and without injection of exogenous dyes. OCTA is based on the fact that stationary tissue generates a time-independent B-scan image, whereas flowing blood motion generates a time-dependent B-scan image.[24-34] That is, if repeated B-scan images of stationary tissue are acquired at the same location over time, then each of the B-scans will be identical. If, however, there is motion in the tissue, caused for example by flowing erythrocytes, then B-scans acquired at the same location but at different times will differ. These differences can be quantitatively described by a decorrelation signal that has the property that large differences (corresponding to fast flow) generate high decorrelation, and small differences (corresponding to slow flow) generate low decorrelation. A number of different techniques for quantitating the decorrelation signal

have been demonstrated.[24-34] Because OCT angiograms are derived from repeated intensity B-scans, they are intrinsically co-registered with structural data. OCTA therefore enables simultaneous assessment of structure and microvasculature.

The retinal and choriocapillaris microvasculature is predominantly oriented along the en face direction, which means dense volumetric scanning of the macula is needed because each pixel in the en face image requires and axial scan. Furthermore, OCTA requires acquisition of repeated B-scans at each location. Taken together, the dense and repeated scanning protocol of OCTA necessitates higher imaging speeds than those used for traditional, structural OCT. The need for ultrahigh imaging speeds has created a gap between the technological development and the clinical application of OCTA, and only recently has OCTA been used to image small numbers of patients with exudative AMD. In 2013, Hong et al published results of 11 eyes with exudative macular disease.[5] In 2014, Schwartz et al reported imaging results from one healthy subject, one patient with dry AMD, one patient with exudative AMD, and one patient with nonproliferative diabetic retinopathy.[35] Also in 2014, Jia et al demonstrated OCTA in the retinas of five healthy participants and five patients with exudative AMD.[6] These prior studies are limited by their relatively small number of patients as well as the small field sizes of the investigative devices used. OCTA is expected to enter the commercial market with the introduction of the 70 kHz Avanti RTVue XR equipped with the prototype AngioVue software (Optovue, Fremont, CA), which will facilitate wider-spread clinical access to OCTA.

Our group has demonstrated ophthalmic swept-source OCT (SS-OCT) using a vertical cavity surface emitting laser (VCSEL) swept light source.[36] Additionally, our group has recently developed a phase-stabilized prototype system with a 400 kHz A-scan rate, approximately five to 10 times faster than standard commercial systems.[37]

The purpose of the present study is to assess the ability of ultrahigh-speed swept-source OCTA to visualize CNV lesions and the underlying choriocapillaris in patients with exudative AMD. Because OCTA enables visualization of co-registered three-dimensional retinal and choroidal microvasculature, it is well-suited for assessing the association between CNV and the underlying choriocapillaris in vivo. Utilizing the ultrahigh 400 kHz A-scan rate, abnormal CNV vasculature and choriocapillaris were simultaneously visualized over wide, 6 mm × 6 mm fields.

Patients and Methods

This study was approved by the institutional review boards at the Massachusetts Institute of Technology (MIT) and Tufts Medical Center. All participants were imaged in the ophthalmology clinic at the New England Eye Center (NEEC) at Tufts Medical Center. Signed written informed consent was obtained from all participants prior to imaging. The research adhered to the tenets of the Declaration of Helsinki and the Health Insurance Portability and Accountability Act. All participants underwent a complete ophthalmic examination including a detailed history, refraction, intraocular pressure measurement, anterior segment examination, and a dilated fundus examination by a general ophthalmologist or a retinal specialist at NEEC. Select patients received color fundus

photography, fundus autofluorescence, FA, and ICGA, as clinically indicated. Healthy participants were defined as having no abnormalities on ophthalmic examination except for an age-appropriate cataract, normal ophthalmic fundus examinations, normal visual fields, refraction less than or equal to 6D, and no history of diabetes.

OCTA was performed with an ultrahigh-speed SS-OCT prototype system developed at MIT and deployed at NEEC in November 2013. A similar OCT system has previously been described in detail,[37] and therefore only key characteristics are summarized here. The instrument used a VCSEL swept light source centered at approximately 1,050 nm wavelength with an approximately 80-nm bandwidth and a 400 kHz A-scan rate. OCT signals were sampled with an analog-to-digital acquisition card externally clocked at a maximum frequency of approximately 1.1 GHz using a Mach-Zehnder interferometer calibration signal; the imaging range was approximately 2.1 mm in tissue. The power incident on the cornea was approximately 1.8 mW.

Two different field sizes were used for OCTA in this study: 6 mm × 6 mm and 3 mm × 3 mm. OCTA data were acquired using five repeated B-scans, each B-scan consisting of 500 A-scans, at 500 individual B-scan locations covering the field size. Each OCTA volume therefore consisted of 2,500 B-scans or 500 × 5 × 500 A-scans. With an A-scan rate of 400 kHz and a galvanometer duty cycle of 80% to 85%, the total image acquisition time was approximately 3.9 seconds per volume. For the 6 mm × 6 mm field size, the volumetric scan pattern of 500 × 500 × 5 A-scans correspond to an isotropic sampling of the retina at a 12-μm interval in the transverse direction. Smaller field sizes yield proportionally denser transverse sampling, providing higher OCT angiogram quality. The interscan time between sequential B-scans was approximately 1.5 ms, and the time required to acquire each B-scan was approximately 7.5 ms (approximately 1.5 ms × 5) per line for all field sizes.

OCT angiograms were generated by computing the speckle decorrelation between standard intensity B-scans that were acquired sequentially from the same location. In particular, the decorrelation between the first and second acquired B-scans was computed, thereby generating one OCT angiogram; the decorrelation between the second and third acquired B-scans was computed, thereby generating another OCT angiogram, and so forth. Using this methodology, our set of five repeated B-scans generated four angiograms, which were averaged into a single OCT angiogram to improve the signal-to-noise ratio. Prior to computing speckle decorrelation, repeated intensity B-scans were registered using a previously described algorithm.[38]

Three-dimensional volumetric OCT angiograms, containing both the retinal and choroidal vasculature, were generated. In order to separately visualize the retinal and choriocapillaris microvasculature, Bruch's membrane and internal limiting membrane (ILM) were semi-automatically segmented using intensity B-scans. Exploiting the co-registration property of the intensity and angiographic data allow the segmentation contours from the structural volume to be directly applied to the angiographic volume. En face retinal OCT angiograms were then created by maximum projection between the ILM and the Bruch's membrane. En face choriocapillaris angiograms were created by selecting a single en face plane,

approximately 4.4 μm in thickness, immediately below Bruch's membrane. CNV was visualized by maximum projection of the en face planes that spanned the CNV.

When describing choriocapillaris OCT angiograms, we made use of the following terminology. The term “flow impairment” was used to refer to a reduction in blood flow, as manifested by a reduced decorrelation signal. The term “atrophy” was used to refer to a loss of vasculature. Atrophy, like flow impairment, also manifests as a reduced decorrelation signal and therefore cannot always be differentiated on OCTA. Finally, the term “choriocapillaris alteration” was used to refer collectively to both atrophy and flow impairment.

Results

Thirty-two healthy participants without ocular disease and 15 patients with CNV were imaged for this study.

Healthy Participants

The group of healthy participants recruited for the study had a mean age (± SD) of 40.7 ± 14.1 years (range: 19 to 70 years; 63 eyes of 32 participants). Among the 63 eyes imaged, 33 were from participants 40 years or older and seven were from participants 60 years or older. Figure 1 shows representative retinal and choriocapillaris angiograms from a 35-year-old healthy participant and a 68-year-old healthy participant. In general, we observed no obvious trend between the integrity of the retinal or choriocapillaris vasculature and participant age for our cohort. None of the healthy participants had OCT angiograms indicating CNV.

Exudative AMD

The group of patients with exudative AMD recruited for the study had a mean age (± SD) of 79.7 ± 8.3 years (range: 61 to 92 years; 19 eyes of 15 patients). Figure 2 (page 500) shows OCT and OCTA images from an 87-year-old patient with treatment-naive exudative AMD with a minimally classic CNV. All images were obtained from a single volumetric scan. FA and ICGA acquired from the same patient are also shown for comparison. The early-stage FA (Figure 2F) shows a sharply demarcated area of hyperfluorescence, which corresponds to the classic component of the lesion. The early-phase ICGA (Figure 2G) shows the occult component of the lesion, which by reference to Figure 2K is determined to be a fibrovascular pigment epithelial detachment (FVPED). In the late-stage FA image (Figure 2H), the continued pooling of fluorescein has obscured the boundaries of the classic component of the lesion, and a stippled hyperfluorescence pattern is seen in the region of the occult component. It is interesting to note that the OCTA projection in Figure 2E reveals the detailed vasculature of both the occult (outlined red) and classic (outlined yellow) components of the lesion, while such detail is not visible in the FA and ICGA images (Figures 2F-H). The multiple white horizontal lines in Figure 2E result from patient eye motion artifacts, which cause transient increases in decorrelation. Although the retinal angiogram in Figure 2B appears relatively normal, the choriocapillaris angiogram in Figure 2D reveals severe choriocapillaris alteration, indicating flow impairment and/or atrophy.

Note that the CNV casts angiographic shadows that make the region under the CNV appear to have circulation when in actuality it does not. Upon closer examination, the region of CNV is seen to be encircled by a “halo” of choriocapillaris alteration. To be sure that the areas of low decorrelation in Figure 2D really correspond to choriocapillaris alteration and not attenuation of the OCT beam, the corresponding intensity slice (Figure 2C) is shown for comparison. The white dashed contour of Figure 2C outlines generously an area of relatively lower intensity signal; this same contour is superimposed on Figure 2D. One can see that there are areas of low decorrelation outside of the contour, which suggests that the low decorrelation is not due to beam attenuation but to flow impairment and/or atrophy. It is likely that the darker regions in Figure 2D are actually regions of choriocapillaris atrophy. The thickness map of Figure 2I shows a region of elevation that corresponds to the FVPED. The OCTA cross-sectional image in Figure 2J, at the position of the white dashed horizontal line in Figure 2E, clearly shows both the occult (outlined red) and the classic (outlined yellow) components of the lesion. The white bracket of Figure 2J roughly indicates the axial depths of the OCTA B-scan that are predominantly composed of shadowing artifacts from the choriocapillaris and choroidal vasculature.

Additional representative OCT angiograms from five exudative AMD cases are shown in Figure 3 (page 502). Note the varied structure and size of the lesions. With reference to the third row, choriocapillaris alteration is visible underneath and surrounding the lesion. To verify that the regions of choriocapillaris alteration are not caused by attenuation of the OCT beam, the corresponding intensity slices are shown in the second row. En face OCT and OCTA slices 35 μm below the choriocapillaris are shown in the fourth and fifth rows, respectively. Low decorrelation at this depth indicates altered choriocapillaris and choroidal vasculature above. The occult (red) and classic (yellow) classifications were determined using the intensity and OCTA B-scans shown in the sixth and seventh rows, respectively.

Of 19 eyes with exudative AMD, CNV was clearly visualized with OCTA in 16 eyes. Among the three eyes in which OCTA did not visualize CNV, one was due to severe subretinal hemorrhage that attenuated the OCT signal completely. The other two eyes had inactive exudative AMD after anti-VEGF treatment as confirmed by the absence of subretinal fluid and pigment epithelial detachment, as well as at least 12 weeks of follow-up without treatment and with no recurrence of subretinal fluid. Therefore, OCTA could visualize 16 of 17 eyes with active CNV, corresponding to a 94% sensitivity for CNV detection. In all, the 16 eyes having CNV that was detectable under OCTA imaging, the CNV originated from regions of severe choriocapillaris alteration. We further observed that in 14 of these eyes, the CNV lesions were surrounded by a region of severe choriocapillaris alteration (Figure 3, page 502). This observation included CNV lesions with longest dimensions ranging from less than 500 μm to greater than 5 mm. In the two eyes in which the CNV was not surrounded by choriocapillaris alteration, the CNV originated from the margin of geographic atrophy (GA) or peripapillary atrophy and grew away from the atrophic region.

Discussion

All CNV lesions that were detectable on OCTA were found to be associated with regions of choriocapillaris alteration, either corresponding to flow impairment and/or atrophy. This finding is consistent with the previous OCTA study by Jia et al, which found some focal regions adjacent to the CNV having a complete absence of choriocapillaris.[6] Using our large, 6 mm × 6 mm field size, we were able to image the entirety of the CNV lesions, which in some cases measured up to 5 mm in maximal diameter, and observed that in 14 of the 16 eyes, the choriocapillaris alteration was present not only underneath the lesion but extended beyond the borders of the CNV, encircling it. Due to the shadowing artifact that the CNV lesion creates on the choriocapillaris en face OCT angiograms, the choriocapillaris alteration beneath the CNV is relatively difficult to visualize. The effect of this shadowing is that the choriocapillaris alteration appears as a ring, or halo, surrounding the boundaries of the lesion. Although more comprehensive longitudinal studies are needed, these findings suggest that CNV lesions may form in regions of choriocapillaris alteration in order to compensate for the reduced circulation. This suggestion was also made by Jia et al and is consistent with the published histopathologic literature.[6,19-21] In a landmark paper by Bhutto and Lutty, the observation was made that in patients with exudative AMD, the CNV lesion occurred in areas of choriocapillaris alteration and the size of the region of choriocapillaris alteration consistently extended beyond the margins of CNV.[19] Bhutto and Lutty also reported that, unlike in GA, the RPE overlying the choriocapillaris was intact. The authors hypothesized that ischemia, due to choriocapillaris loss, caused the RPE to release vasogenic factors, including VEGF, which in turn resulted in CNV. In another study, CNV was found to develop at the peripheral border of GA and/or at the region of foveal sparing and was never found to develop in the region of RPE atrophy.[39] This is consistent with the findings of our study where, in the two patients with GA, the CNV occurred at the margins of atrophy and appeared to grow away from the atrophy. As mentioned by Bhutto and Lutty, this growth pattern suggests that the RPE cells may provide the stimulus for CNV formation.[19]

Compared with conventional dye-based angiography techniques, OCTA offers several distinct advantages. First, OCTA does not require the injection of exogenous dyes and is noninvasive. Second, unlike dye-based angiography, OCTA is fast (typical acquisition time: < 4 seconds), and can be performed at any time and potentially during every patient visit. Third, OCTA enables depth-resolved imaging of both the retinal and choroidal vasculature. Taken together, these advantages provide a strong argument for OCTA imaging of the retinal and choroidal microvasculature, particularly in longitudinal studies. It should also be noted that we found OCTA to be capable of visualizing classic and occult lesions with equal clarity, a finding that is consistent with the results of Jia et al.[6]

Unlike dye-based angiography, OCTA does not visualize leakage. Although this may be a limitation for the investigation of retinal pathologies involving alterations in vascular permeability, it also has certain advantages. For example, while leakage of CNV in exudative AMD is used to confirm the existence of CNV, leakage produces hyperfluorescence that can impair visibility and make detection of angiographic features of the CNV lesion difficult. These difficulties are further compounded by a lack of depth

resolution in dye-based techniques. In contrast, OCTA directly visualizes abnormal vasculature in three dimensions and therefore may be useful for monitoring treatment response. Furthermore, because there is no obscuring hyperfluorescence from dye leakage, OCTA can better visualize the choriocapillaris than dye-based methods. In our study, OCTA visualized the CNV lesion in 16 of the 17 patients with active exudative AMD. The only case in which OCTA failed to visualize the lesion was due to significant subretinal hemorrhage attenuating the OCT signal. Even in that case, however, subretinal fluid was visible as a marker in structural OCT images.

At this point it is clear that a certain degree of care must be taken when interpreting OCTA images. First, vasculature can cast angiographic shadows onto the layers below. One example of this is the shadows of the retinal vasculature that appear in the choriocapillaris OCT angiograms. Another example is the shadows that the choriocapillaris and choroidal vasculature cast onto the deeper layers. Regarding the latter, consider the OCTA B-scan of Figure 2J (page 500). The bracket indicates the depths of the OCT angiogram that are predominantly uninterpretable due to angiographic shadowing from the choriocapillaris and choroidal vasculature above. To say, however, that the OCT angiogram at these depths is completely uninterpretable is incorrect. First, the decorrelation function can be altered to reduce shadowing at the expense of a decreased ability to detect slow flows; this is not the approach that we employed in the present work. Second, at depths below the choriocapillaris, the absence of a decorrelation signal can provide useful information. In particular, the absence of decorrelation at depths below the choriocapillaris indicates the presence of overlying choriocapillaris or choroidal vasculature. We used this property to confirm choriocapillaris alteration, as discussed below.

As noted previously, en face images of the choriocapillaris were attained by segmenting Bruch's membrane and then selecting the en face slice immediately below. Because the choriocapillaris is a thin monolayer network of capillaries (the capillaries have an axial diameter of approximately 6.5 to 10 μm in normal maculae), accurate segmentation is of utmost importance.[40,41] Errors in segmentation will result in the inclusion of regions out of the plane of the choriocapillaris (ie, above or below the choriocapillaris) in the en face choriocapillaris angiogram. When regions above the choriocapillaris are included, normal choriocapillaris can appear as altered; when regions below are included, altered choriocapillaris can appear as normal. We primarily care about the former: that is, ensuring that we are not interpreting normal choriocapillaris as altered choriocapillaris. To mitigate this possibility, the fourth and fifth rows of Figure 3 show en face intensity and OCTA slices 35 μm below the choriocapillaris slices of the second and third rows. The rationale is that even if there are segmentation inaccuracies, by going 35 μm below the segmented choriocapillaris, we ensure that we are below or at the very least in the choriocapillaris. At this depth, if there were normal choriocapillaris and choroidal vasculature above, shadowing artifacts would be present and the OCT angiogram would appear highly decorrelated. Thus, any regions of low decorrelation at this depth correspond to regions of choriocapillaris alteration above. Inspecting the fifth row of Figure 3, we can see that even at 35 μm below the segmented choriocapillaris, there are regions of low decorrelation. These regions correspond to regions of choriocapillaris alteration above. Finally, note that the implication is one-way: low decorrelation at depths below the choriocapillaris corresponds to

choriocapillaris alteration above, but high decorrelation at depths below the choriocapillaris does not necessarily correspond to healthy choriocapillaris above. This is because even when the choriocapillaris is altered, choroidal vasculature may be present and cast shadows.

Our decision to use the terms choriocapillaris alteration, flow impairment, and atrophy merits some discussion. The decorrelation signal is obtained by comparing B-scans that are sequentially acquired from the same location. The sequentially acquired B-scans are separated by a time interval, which we call the interscan time. The longer the interscan time, the larger the decorrelation signal because the erythrocytes will have moved a larger distance in between scans. The interscan time determines the fastest distinguishable flow and slowest detectable flow that can be measured using OCTA. Simply stated, certain flows are fast enough to saturate the decorrelation signal, meaning that they can no longer be distinguished from one another; we say that these flows are faster than the fastest distinguishable flow. Note that the smaller the interscan time, the faster the fastest distinguishable flow. There are also certain flows in which the erythrocytes move slowly enough to only shift a very small distance during the interscan time. These flows generate decorrelation signals below the detection level; we say that these flows are slower than the slowest detectable flow. Our usage of the terms choriocapillaris alteration, flow impairment, and atrophy reflects an ambiguity when interpreting an OCT angiogram. In particular, a region of low decorrelation signal could be due to either atrophy (a complete absence of flow) or flow impairment (where flow is present but slower than the slowest detectable flow). In this study, we have been careful to interpret a low decorrelation signal as being possibly caused by either flow impairment or atrophy. It is possible, by modulating the interscan times, to distinguish between flow impairment and atrophy; however due to its complexity, we did not pursue this approach in the current study.

A limitation of the current study is that the number of healthy eyes was small and the mean age of the healthy participants was lower than that of the CNV group. Choriocapillaris alteration was not observed in any of the seven eyes from healthy participants aged 70 years or older in this study. Further investigation is, however, required to determine whether an older cohort of healthy participants would show significant choriocapillaris alteration. In the future, a more comprehensive cohort of age-matched healthy participants needs to be recruited.

Despite this limitation, this study strongly suggests that the advantages of OCTA may make it widely useful for noninvasive monitoring of the retinal and choriocapillaris microvasculature in patients with CNV. This monitoring may in turn assist in the diagnosis of CNV as well as the monitoring of its progress and response to therapy.

Acknowledgments

Dr. Duker is a consultant for Carl Zeiss Meditec and Optovue and has stock in Hemera Biosciences, EyeNetra, and Ophthotech. Dr. Fujimoto has received royalties from intellectual property owned by Massachusetts Institute of Technology and licensed to Carl Zeiss Meditec and Optovue and has stock options with Optovue. Dr. Rosenfeld has received research support from Carl Zeiss Meditec.

References

1. Rosenfeld PJ, Moshfeghi AA, Puliafito CA. Optical coherence tomography findings after an intravitreal injection of bevacizumab (Avastin) for neovascular age-related macular degeneration. Ophthalmic Surg Lasers Imaging Retina. 2005; 36(4):331–335.
2. Kaiser PK, Blodi BA, Shapiro H, et al. Angiographic and optical coherence tomographic results of the MARINA study of ranibizumab in neovascular age-related macular degeneration. Ophthalmology. 2007; 114(10):1868–1875. [PubMed: 17628683]
3. Fung AE, Lalwani GA, Rosenfeld PJ, et al. An optical coherence tomography-guided, variable dosing regimen with intravitreal ranibizumab (lucentis) for neovascular age-related macular degeneration. Am J Ophthalmol. 2007; 143(4):566–583. [PubMed: 17386270]
4. Lalwani GA, Rosenfeld PJ, Fung AE, et al. A variable-dosing regimen with intravitreal ranibizumab for neovascular age-related macular degeneration: year 2 of the PrONTO Study. Am J Ophthalmol. 2009; 148(1):43–58. [PubMed: 19376495]
5. Hong YJ, Miura M, Makita S, et al. Noninvasive investigation of deep vascular pathologies of exudative macular diseases by high-penetration optical coherence angiography. Invest Ophthalmol Vis Sci. 2013; 54(5):3621–3631. [PubMed: 23633664]
6. Jia Y, Bailey ST, Wilson DJ, et al. Quantitative optical coherence tomography angiography of choroidal neovascularization in age-related macular degeneration. Ophthalmology. 2014; 121(7): 1435–1444. [PubMed: 24679442]
7. Albert, DM.; Miller, JW.; Azar, DT.; Blodi, BA. Albert & Jakobiec's Principles & Practice of Ophthalmology. 3rd. Philadelphia, PA: Saunders Elsevier; 2008.
8. Ryan, S.; Schachat, A.; Wilkinson, C., et al. Retina. 5th. Philadelphia, PA: Saunders Elsevier; 2013.
9. Bressler NM, Doan QV, Varma R, et al. Estimated cases of legal blindness and visual impairment avoided using ranibizumab for choroidal neovascularization: non-Hispanic white population in the United States with age-related macular degeneration. Arch Ophthalmol. 2011; 129(6):709–717. [PubMed: 21670337]
10. Gragoudas ES, Adamis AP, Cunningham ET, et al. Pegaptanib for neovascular age-related macular degeneration. New Engl J Med. 2004; 351(27):2805–2816. [PubMed: 15625332]
11. Brown DM, Kaiser PK, Michels M, et al. Ranibizumab versus verte-porfn for neovascular age-related macular degeneration. New Engl J Med. 2006; 355(14):1432–1444. [PubMed: 17021319]
12. Rosenfeld PJ, Brown DM, Heier JS, et al. Ranibizumab for neovascular age-related macular degeneration. New Engl J Med. 2006; 355(14):1419–1431. [PubMed: 17021318]
13. Schmidt-Erfurth UM, Pruente C. Management of neovascular age-related macular degeneration. Prog Retin Eye Res. 2007; 26(4):437–451. [PubMed: 17512238]
14. Bressler NM. Antiangiogenic approaches to age-related macular degeneration today. Ophthalmology. 2009; 116(10):S15–S23. [PubMed: 19800535]
15. Martin DF, Maguire MG, Fine SL, et al. Ranibizumab and bevacizumab for treatment of neovascular age-related macular degeneration: two-year results. Ophthalmology. 2012; 119(7): 1388–1398. [PubMed: 22555112]
16. Bischoff P, Flower R. Ten years experience with choroidal angiography using indocyanine green dye: a new routine examination or an epilogue? Doc Ophthalmol. 1985; 60(3):235–291. [PubMed: 2414083]
17. Flower R. Extraction of choriocapillaris hemodynamic data from ICG fluorescence angiograms. Invest Ophthalmol Vis Sci. 1993; 34(9):2720–2729. [PubMed: 8344794]
18. Zhu L, Zheng Y, von Kerczek CH, et al. Feasibility of Extracting Velocity Distribution in Choriocapillaris in Human Eyes from ICG Dye Angiograms. J Biomech Eng. 2005; 128(2):203–209. [PubMed: 16524331]
19. Bhutto I, Lutty G. Understanding age-related macular degeneration (AMD): Relationships between the photoreceptor/retinal pigment epithelium/Bruch's membrane/choriocapillaris complex. Mol Aspects Med. 2012; 33(4):295–317. [PubMed: 22542780]
20. McLeod DS, Taomoto M, Otsuji T, et al. Quantifying changes in RPE and choroidal vasculature in eyes with age-related macular degeneration. Invest Ophthalmol Vis Sci. 2002; 43(6):1986–1993. [PubMed: 12037009]

21. McLeod DS, Grebe R, Bhutto I, et al. Relationship between RPE and choriocapillaris in age-related macular degeneration. Invest Ophth Vis Sci. 2009; 50(10):4982–4991.
22. Fein JG, Branchini LA, Manjunath V, et al. Analysis of short-term change in subfoveal choroidal thickness in eyes with age-related macular degeneration using optical coherence tomography. Ophthalmic Surg Lasers Imaging Retina. 2014; 45(1):32–37. [PubMed: 24392909]
23. Kim S, Oh J, Kwon S, et al. Comparison of Choroidal Thickness among Patients with Healthy Eyes, Early Age-Related Maculopathy, Neovascular Age-Related Macular Degeneration, Central Serous Chorioretinopathy, and Polypoidal Choroidal Vasculopathy. Retina-J Ret Vit Dis. 2011; 31(9):1904–1911.
24. Makita S, Hong Y, Yamanari M, et al. Optical coherence angiography. Opt Express. 2006; 14(17): 7821–7840. [PubMed: 19529151]
25. Fingler J, Schwartz D, Yang CH, et al. Mobility and transverse flow visualization using phase variance contrast with spectral domain optical coherence tomography. Opt Express. 2007; 15(20): 12636–12653. [PubMed: 19550532]
26. Tao YK, Davis AM, Izatt JA. Single-pass volumetric bidirectional blood flow imaging spectral domain optical coherence tomography using a modified Hilbert transform. Opt Express. 2008; 16(16):12350–12361. [PubMed: 18679512]
27. An L, Wang RKK. In vivo volumetric imaging of vascular perfusion within human retina and choroids with optical micro-angiography. Opt Express. 2008; 16(15):11438–11452. [PubMed: 18648464]
28. Mariampillai A, Standish BA, Moriyama EH, et al. Speckle variance detection of microvasculature using swept-source optical coherence tomography. Opt Lett. 2008; 33(13):1530–1532. [PubMed: 18594688]
29. Vakoc BJ, Lanning RM, Tyrrell JA, et al. Three-dimensional microscopy of the tumor microenvironment in vivo using optical frequency domain imaging. Nat Med. 2009; 15(10):1219–1223. [PubMed: 19749772]
30. Yu LF, Chen ZP. Doppler variance imaging for three-dimensional retina and choroid angiography. J Biomed Opt. 2010; 15(1):1–4.
31. Jonathan E, Enfield J, Leahy MJ. Correlation mapping: rapid method for retrieving microcirculation morphology from optical coherence tomography intensity images. P Soc Photo-Opt Ins. 2011; 7898(1):1–5.
32. Blatter C, Klein T, Grajciar B, et al. Ultrahigh-speed non-invasive widefield angiography. J Biomed Opt. 2012; 17(7):1–4.
33. Jia YL, Tan O, Tokayer J, et al. Split-spectrum amplitude-decorrelation angiography with optical coherence tomography. Opt Express. 2012; 20(4):4710–4725. [PubMed: 22418228]
34. Choi W, Mohler KJ, Potsaid B, et al. Choriocapillaris and choroidal microvasculature imaging with ultrahigh speed OCT angiography. PLOS ONE. 2013; 8(12):e81499. [PubMed: 24349078]
35. Schwartz DM, Fingler J, Kim DY, et al. Phase-variance optical coherence tomography: a technique for noninvasive angiography. Ophthalmology. 2014; 121(1):180–187. [PubMed: 24156929]
36. Grulkowski I, Liu JJ, Potsaid B, et al. Retinal, anterior segment and full eye imaging using ultrahigh speed swept source OCT with vertical-cavity surface emitting lasers. Biomed Opt Express. 2012; 3(11):2733–2751. [PubMed: 23162712]
37. Choi W, Potsaid B, Jayaraman V, et al. Phase-sensitive swept-source optical coherence tomography imaging of the human retina with a vertical cavity surface-emitting laser light source. Opt Lett. 2013; 38(3):338–340. [PubMed: 23381430]
38. Guizar-Sicairos M, Thurman ST, Fienup JR. Efficient subpixel image registration algorithms. Opt Lett. 2008; 33(2):156–158. [PubMed: 18197224]
39. Sunness JS, Gonzalez-Baron J, Bressler NM, et al. The development of choroidal neovascularization in eyes with the geographic atrophy form of age-related macular degeneration. Ophthalmology. 1999; 106(5):910–919. [PubMed: 10328389]
40. Ramrattan RS, van der Schaft TL, Mooy CM, et al. Morphometric analysis of Bruch's membrane, the choriocapillaris, and the choroid in aging. Invest Ophth Vis Sci. 1994; 35(6):2857–2864.

41. Flower RW, von Kerczek C, Zhu L, et al. Theoretical investigation of the role of choriocapillaris blood flow in treatment of subfoveal choroidal neovascularization associated with age-related macular degeneration. Am J Ophthalmol. 2001; 132(1):85–93. [PubMed: 11438059]

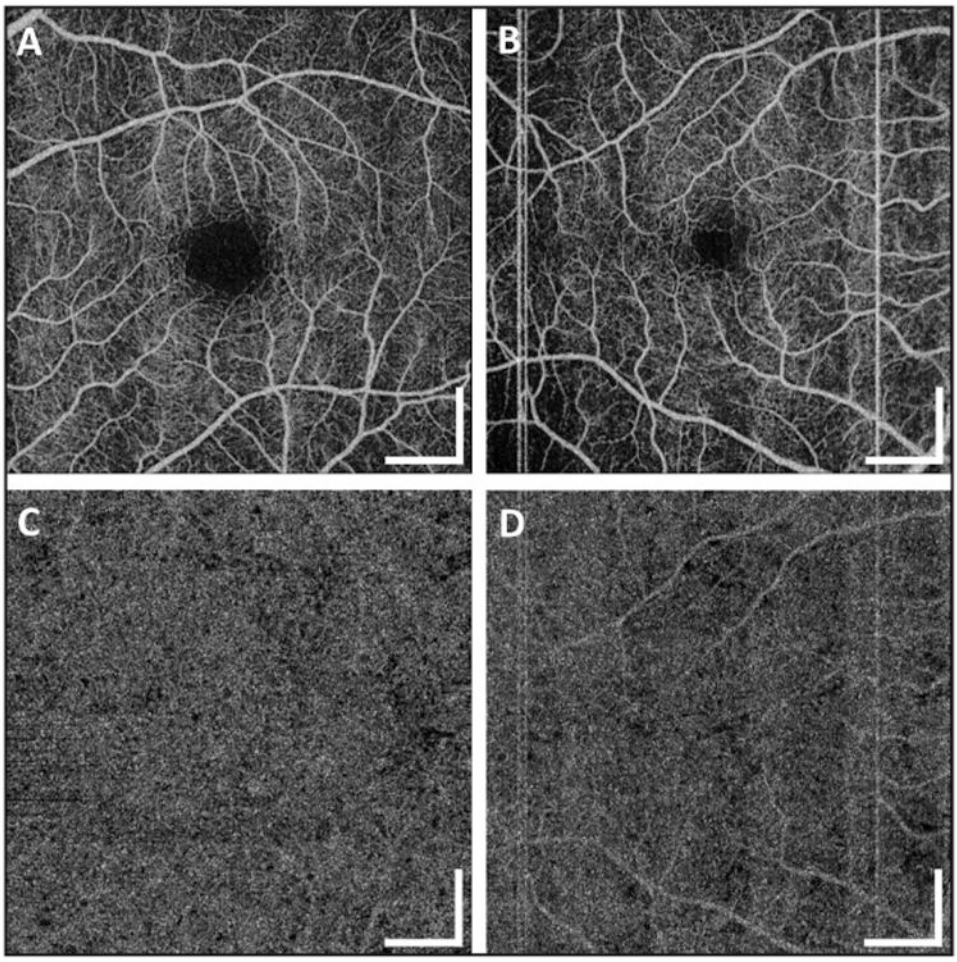

Figure 1.

(A, C) OCT angiograms of a 35-year-old healthy participant. (B, D) OCT angiograms of a 68-year-old healthy participant. (A, B) OCT retinal angiograms over a 6 mm × 6 mm area centered at the fovea. (C, D) OCT choriocapillaris angiograms over the same 6 mm × 6 mm area extracted from the same volumetric scans as used in A and B. Note that the thick retinal vasculature casts angiographic shadows onto the choriocapillaris angiogram. Scale bars: 1 mm.

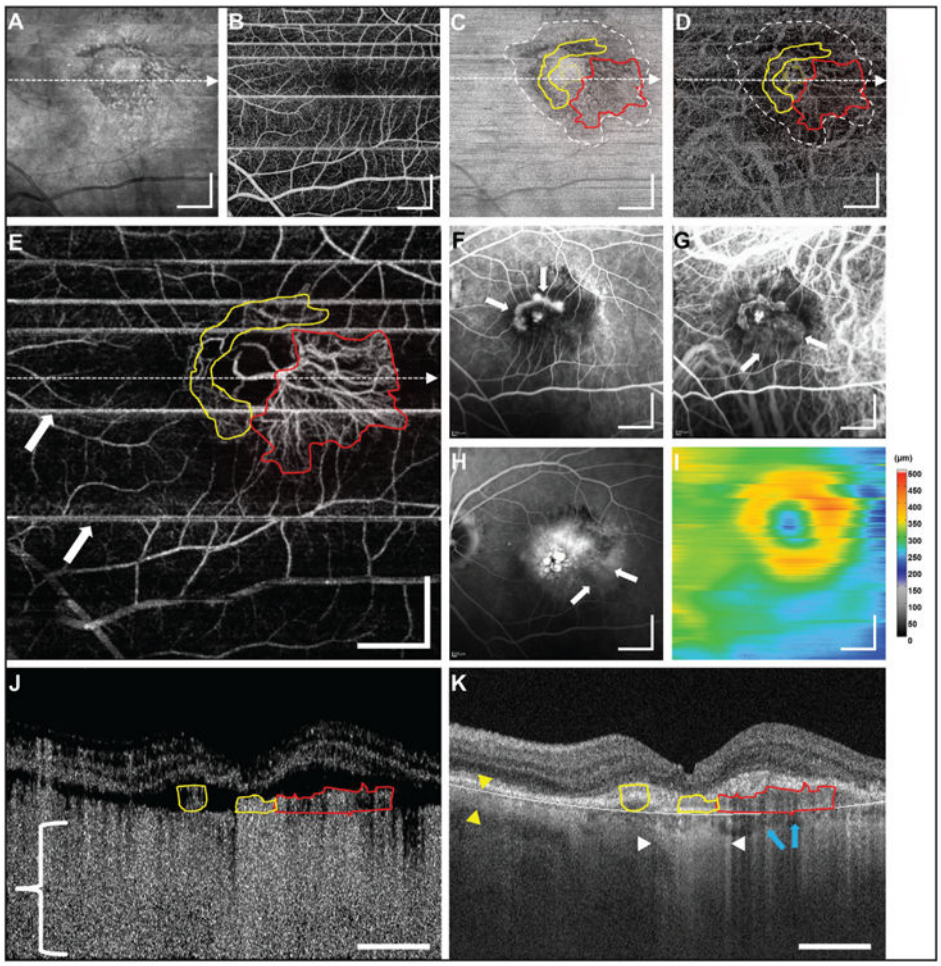

Figure 2.

An 87-year-old patient with a choroidal neovascularization (CNV) lesion exhibiting both occult and classic components. (A) En face mean projection of entire OCT intensity volume. (B) En face projection of the OCT angiogram volume through the depths spanned by the retinal vasculature. (C) En face slice of the OCT intensity volume at the depth of the choriocapillaris. The white dashed contour encircles an area of lower intensity. (D) En face slice of the OCT angiogram volume at the depth of the choriocapillaris. (E) En face projection of the OCT angiogram volume through the depths spanned by the CNV. The red outlining corresponds to the occult components of the lesion, while the yellow outlining corresponds to the classic components. The arrows point to motion artifacts that appear as straight white lines through the image. (F) Early-phase FA. Arrows point to the classic component. (G) Early-phase ICGA. Arrows point to the occult component. (H) Late-phase FA. Arrows point to area of stippled hyperfluorescence. (I) OCT retinal thickness map. (J-K) OCT intensity and OCT angiogram cross-sections, respectively, corresponding to the white dashed horizontal lines in (E). The bracket in (J) roughly spans the depths in which the OCT angiogram B-scan is uninterpretable due to shadowing from the choriocapillaris and choroidal vasculature above. The yellow arrows in K indicate the thickness of the choroid away from the lesion, the white arrows demarcate an area of increased light penetration due to RPE atrophy, and the blue arrows correspond to a region of shadowing from the CNV

lesion. All OCT images are from a 6 mm × 6 mm area, and all scale bars are 1 mm. All OCT and OCT angiogram images were generated from a single volumetric scan.

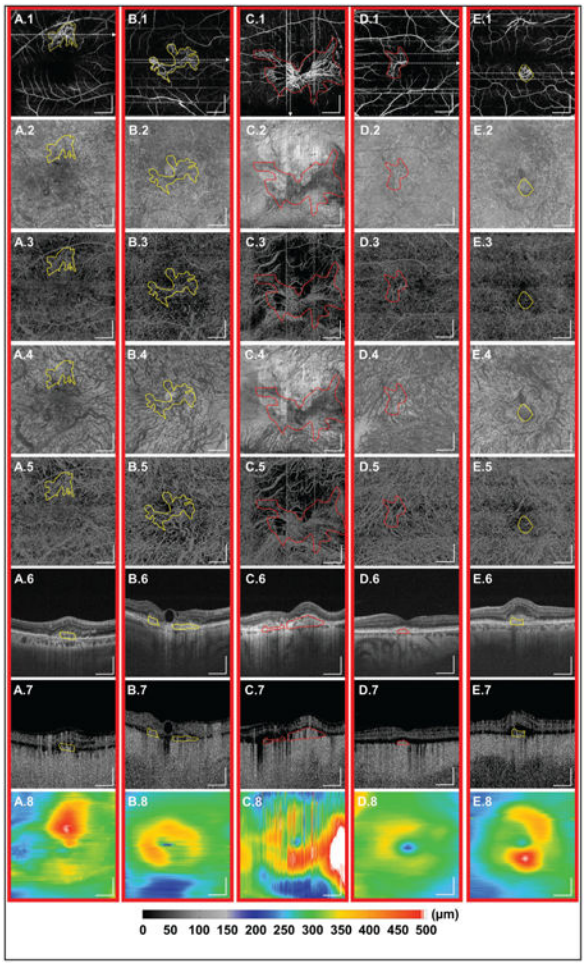

Figure 3.

(A-E) Each column corresponds to a different exudative CNV patient. Row 1 displays en face projections of the OCTA volumes through the depths spanned by the CNV. The lesions are indicated by yellow/red outlining. Yellow outlining corresponds to a component that is suspected to be classic; red outlining corresponds to a component that is suspected to be occult. Row 2 shows en face slices of the OCT intensity volume at the depth of the choriocapillaris; row 3 shows the corresponding en face slices of the OCTA volume. Row 4 shows en face slices of the OCT intensity volume at 35 μm beneath the choriocapillaris; row 5 shows the corresponding en face slices of the OCTA volume which shows OCTA shadowing from the choriocapillaris. Rows 6 and 7 show intensity and angiography B-scans, respectively, corresponding to the horizontal and vertical dashed white lines of the first row. The white contour of the row 6 shows the segmentation of Bruch's membrane. Row 8 shows OCT retinal thickness maps. All images were acquired from 6 mm × 6 mm areas. All scale bars are 1 mm.